

Nanoscale

Accepted Manuscript



This is an *Accepted Manuscript*, which has been through the Royal Society of Chemistry peer review process and has been accepted for publication.

Accepted Manuscripts are published online shortly after acceptance, before technical editing, formatting and proof reading. Using this free service, authors can make their results available to the community, in citable form, before we publish the edited article. We will replace this *Accepted Manuscript* with the edited and formatted *Advance Article* as soon as it is available.

You can find more information about *Accepted Manuscripts* in the [Information for Authors](#).

Please note that technical editing may introduce minor changes to the text and/or graphics, which may alter content. The journal's standard [Terms & Conditions](#) and the [Ethical guidelines](#) still apply. In no event shall the Royal Society of Chemistry be held responsible for any errors or omissions in this *Accepted Manuscript* or any consequences arising from the use of any information it contains.

Cite this: DOI: 10.1039/c0xx00000x

www.rsc.org/xxxxxx

ARTICLE TYPE

Adsorption-geometry induced transformation of self-assembled nanostructures of an aldehyde molecule on Cu(110)

Chi Zhang,[‡] Qiang Sun,[‡] Kai Sheng, Qinggang Tan, and Wei Xu*

Received (in XXX, XXX) Xth XXXXXXXXXX 20XX, Accepted Xth XXXXXXXXXX 20XX

DOI: 10.1039/b000000x

From an interplay of high-resolution STM imaging/manipulation and DFT calculations, we have revealed that different self-assembled nanostructures of BA molecule on Cu(110) are attributed to specific molecular adsorption geometries and thus the corresponding intermolecular hydrogen bonding patterns, and the STM manipulations demonstrate the feasibility of switching such weak-hydrogen-bonding patterns.

Supramolecular architectures from molecular self-assembly on solid surfaces have aroused significant attentions due to the attached new functionalities and a multitude of potential applications in, e.g. biochemical sensors, chiral catalysis, and organic electronics¹⁻³. One prerequisite to achieve well-defined nanostructures is an exhaustive exploration of the influencing factors dominating the whole self-assembly processes. As for intrinsic factors, different kinds of intermolecular interactions typically involving functional groups such as nitrile⁴⁻⁶, amine⁷⁻⁸ and carboxyl group⁹⁻¹⁰ have been extensively explored and well-ordered nanostructures have been achieved. Also, external stimuli, such as STM manipulations¹¹⁻¹³, UV irradiation¹⁴, have proved to be effective ways to influence the self-assembled nanostructures. However, to our knowledge, on-surface self-assembly of an aldehyde molecule has been rarely reported^{15,16} and in-depth exploration and controllable switch of intermolecular interactions in relation to molecular adsorption geometries has not been particularly emphasized. Understanding the details of molecular self-assembly and forced-assembly processes may shed light on designing man-made molecular nanostructures.

In this work, we have explored the self-assembly of an aromatic aldehyde molecule (Biphenyl-4-carboxaldehyde (shortened as BA)) on the Cu(110) substrate under ultrahigh vacuum (UHV) conditions. From an interplay of high-resolution scanning tunneling microscopy (STM) imaging/manipulation and density functional theory (DFT) calculations, we have investigated the self-assembly of BA molecules at various coverages where different intermolecular hydrogen bonding patterns in relation to molecular adsorption geometries are explored in depth. At low coverage, we found that BA molecules prefer to adsorb on the surface in two specific directions (i.e. $\pm 35^\circ$ with respect to [001] direction of the substrate) and form discrete clusters typically as windmill-like tetramers bound by weak intermolecular hydrogen bonds. At high coverage (~ 1 ML), we found the formation of well-ordered close-packed molecular

nanostructures, and interestingly, inside the structures some specific BA molecules exhibited one additional adsorption direction (i.e. along [001] direction) resulting from molecular packing and different hydrogen bonding patterns. By in-situ STM manipulations, we surprisingly found that the hydrogen bonding pattern appeared in the high-coverage structure could be artificially achieved in the low-coverage one. These results demonstrate the versatility of weak hydrogen bonding in the fabrication of on-surface molecular nanostructures and the capability of STM manipulation technique in switching intermolecular hydrogen bonding patterns, which may be extended into more complicated systems with the aim of designing functional nanostructures via bottom-up strategy.

The STM experiments were performed in a UHV chamber (base pressure 1×10^{-10} mbar) equipped with a variable-temperature "Aarhus-type" STM purchased from SPECS^{17,18}, a molecular evaporator and standard facilities for sample preparation. After the system was thoroughly degassed, the molecules were deposited by thermal sublimation onto a Cu(110) substrate. The sample was thereafter transferred within the UHV chamber to the STM, where measurements were carried out at ~ 100 K. The lateral manipulations were carried out in a controllable line-scan mode under specific scanning conditions (by increasing the tunnel current up to approximately 2.0 nA while reducing the tunnel voltage down to approximately 20 mV^{19,20}). All the calculations were carried out in the framework of DFT by using the Vienna ab-initio simulation package (VASP)^{21,22}. The projector augmented wave method was used to describe the interaction between ions and electrons^{23,24}. We employed the PBE-GGA as the exchange correlation functional²⁵ and van der Waals interactions were included using the DFT-D2 method of Grimme²⁶. The atomic structures were relaxed using the conjugate gradient algorithm scheme as implemented in the VASP code until the forces on all unconstrained atoms were ≤ 0.03 eV/Å.

After deposition of BA molecules on the Cu(110) substrate held at RT, we find that the molecules can form discrete clusters in which two specific molecular adsorption directions are identified (cf. Figure 1a), and these clusters are mainly constituted by two kinds of chiral windmill-like tetramers as building blocks as shown by high-resolution STM images (cf. Figure 1b). According to the STM observations, we have carried out systematic structural search by proposing different possible tetramers and finally obtained the energetically most favorable

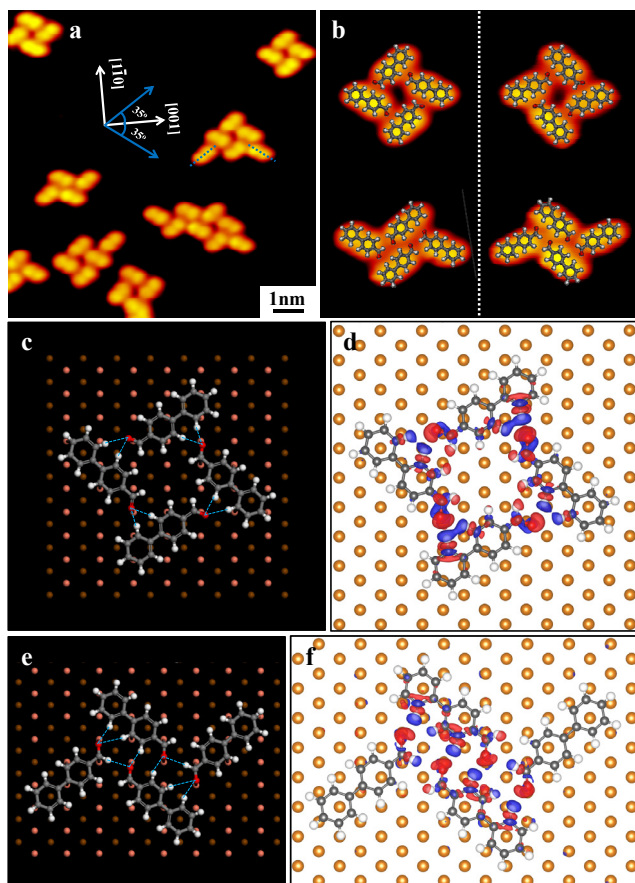


Figure 1. (a) STM image showing the formation of discrete clusters after deposition of BA molecules at a low coverage (~ 0.1 ML) on the Cu(110) substrate held at room temperature (RT). The blue arrows (parallel to the dashed lines) indicate the two adsorption directions of BA molecules (i.e. $\pm 35^\circ$ with respect to the [001] direction). (b) The high-resolution STM images of the typical tetramers with the DFT optimized structural models superimposed. The corresponding enantiomers are separated by white dot line. Scanning conditions: $I_t = 1.38$ nA, $V_t = -1250$ mV. (c) and (e) show the DFT optimized structural models of the two kinds of tetramers including the Cu(110) substrate and the corresponding charge density difference maps (the four molecules on the substrate are considered to be four individual species and the charge transfers between four individual molecules and the substrate have been subtracted) are shown in (d) and (f), respectively. The hydrogen bonds are indicated in blue dot lines in (c) and (e). The isosurface values in (d) and (f) are at the same level of 0.0007 $e/\text{\AA}^3$. Blue and red isosurfaces indicate charge depletion and accumulation, respectively. O: red, C: gray, H: white, first layer Cu atoms: bronze, second layer Cu atoms: brown. Cu atoms in 1d and 1f: golden.

structural models including the substrate as shown in Figure 1c and 1e, which are also superimposed on top of the corresponding close-up STM images, respectively, and good agreements are achieved (cf. Figure 1b). As depicted in Figure 1c and 1e, we can identify that within the tetramer structures the BA molecules interact with each other via different weak C-H \cdots O hydrogen bonds as indicated by the blue dot lines, and the charge density difference maps plotted in Figure 1d and 1f help to further recognize the hydrogen bonding patterns in the tetramer structures.

To further investigate the self-assembly of BA molecules at higher coverages and the interactions among the neighboring BA molecules, we have varied the coverages up to ~ 1 ML (for the coverages at ~ 0.7 - 1.0 ML see Figure S1). Interestingly, after

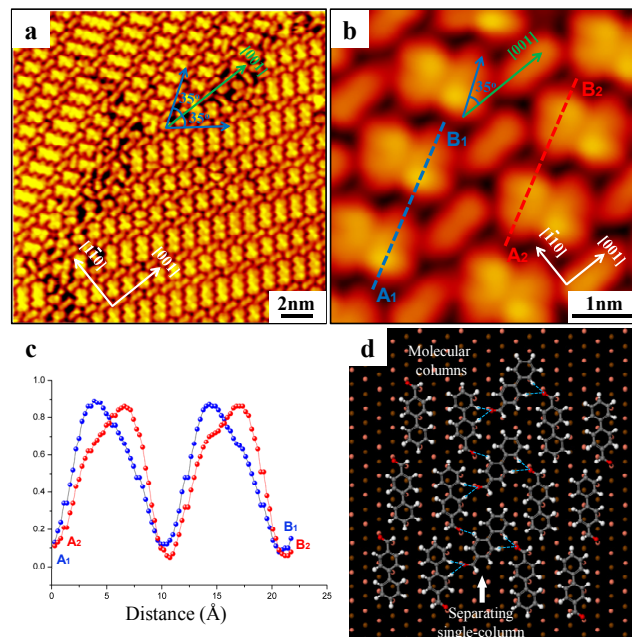


Figure 2. (a) The large-scale STM image showing the formation of the close-packed nanostructure after deposition of BA molecules at a high coverage (~ 1 ML) on the Cu(110) substrate held at RT and subsequent annealing to ~ 370 K for 10 min. The blue arrows and green arrow indicate the two original molecular adsorption directions (i.e. $\pm 35^\circ$ with respect to the [001] direction) and the one additional adsorption direction (i.e. along the [001] direction), respectively. (b) The close-up STM image of the close-packed nanostructure. Scanning conditions: $I_t = 1.24$ nA, $V_t = -2100$ mV. (c) The line-scan profiles along the blue and red dot lines illustrated in (b). (d) The DFT optimized structural model of the typical close-packed nanostructure including the Cu(110) substrate.

deposition of BA molecules at ~ 1 ML coverage on Cu(110) held at RT with subsequent annealing to 370 K, we observe the formation of well-ordered close-packed nanostructures with only two growing directions as shown in Figure 2a. As illustrated in the close-up STM image (cf. Figure 2b), besides the original molecular adsorption directions (i.e. 35° with respect to the [001] direction indicated by the blue arrow, which is consistent with that within the discrete clusters formed at a low coverage), one additional adsorption direction of BA molecule (i.e. along the [001] direction indicated by the green arrow) is observed. The slight difference in apparent topography of the BA molecules along the [001] direction within the close-packed nanostructures may be due to different tip states as in some cases there is no difference (cf. Figure S2). It appears that the molecules with two original adsorption orientations prefer to arrange in a side-by-side mode to form ordered stripes typically ranging from two to four columns (more columns exist as well) (cf. Figure S3, S4) which are always alternately separated by single-column molecules with the molecular adsorption direction along the [001] direction. Interestingly, as illustrated by the line-scan profiles (cf. Figure 2c), we can identify that the left and right neighboring molecules of the single-column molecules adopt an anti-parallel arrangement. Based on the STM indications discussed above, different gas-phase structural models (with the molecular columns typically ranging from two to four) have been optimized and the energetically most favorable ones have been shown in Figure S3 and good agreements are achieved. Furthermore, we

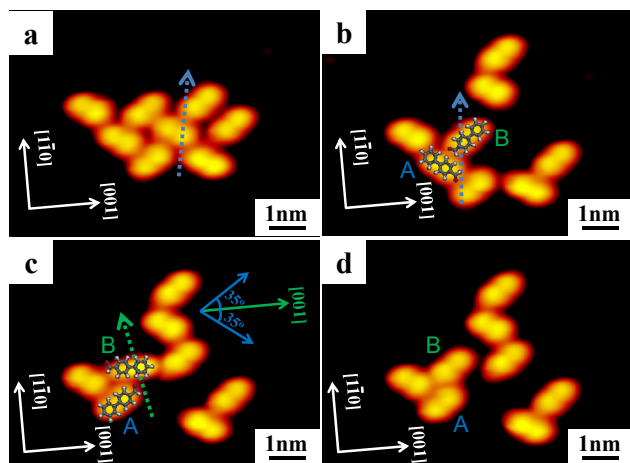


Figure 3. Lateral STM manipulations of the cluster structures formed at a low molecular coverage (~ 0.1 ML). The blue and green arrows in (a), (b) and (c) indicate the directions of STM manipulation. Manipulation conditions: $I_t = 2$ nA, $V_t = 20$ mV, Scanning conditions: $I_t = 1.33$ nA, $V_t = -1250$ mV.

have carried out systematic search on the simplified structure composed of two molecular columns and one separating single-column as the unit cell and we finally obtain the energetically most favorable structural model of the close-packed nanostructure including the substrate as shown in Figure 2d. From the optimized model we can identify that the molecules within the single column interact with the neighboring molecules by a new C-H \cdots O hydrogen bonding pattern. Thus, the main driving forces for the formation and stabilization of the close-packed nanostructures are molecular packing and squeezing (to induce the different molecular adsorption direction, that is, along the [001] direction) at high coverages and then forming the weak hydrogen bonds between the single-column molecules and the neighboring molecules at the two sides. The anti-parallel arrangement of the neighboring molecules beside the single molecular column just results from such intermolecular interaction. The intermolecular forces within the side-by-side molecular columns are mainly van der Waals (vdW) interaction.

To unravel the nature of the differences between the two self-assembled nanostructures (i.e. the discrete clusters and the close-packed structures) and explore the possibility of switching different hydrogen bonding patterns, we have performed a series of delicate in-situ STM manipulations as shown in Figure 3. After manipulation of the cluster structure formed at a low molecular coverage (cf. Figure 3a-b), two molecules could be detached from the cluster indicating the relatively weak C-H \cdots O intermolecular hydrogen bonding characteristic. Further manipulation on the remaining cluster (cf. Figure 3b) results in the switching of molecular adsorption geometries of molecule A and B (as marked in Figure 3b) (cf. Figure 3c), that is, molecule A is switched to its symmetric direction with respect to the [001] direction (i.e. $\pm 35^\circ$ with respect to the [001] direction as discussed above), and interestingly, molecule B is switched to the [001] direction which is only observed in the high-coverage nanostructures. Closer inspection of the high-resolution STM images together with the superimposed molecular models (which correspond to the structural models as shown in Figure 1c and Figure 2d, respectively) (cf. Figure 3b-c) allows us to identify that such

STM manipulation actually results in the switching of different hydrogen bonding patterns from the one formed in the tetramer structure at a low coverage (cf. Figure 1c) to the one formed in the close-packed structure at a high coverage (cf. Figure 2d). Also the adsorption geometry of molecule B can be switched back to the original one (cf. Figure 3c-d).

In conclusion, from an interplay of high-resolution STM imaging/manipulation and DFT calculations, we have revealed that different self-assembled nanostructures of BA molecule on Cu(110) are attributed to specific molecular adsorption geometries and thus the corresponding intermolecular hydrogen bonding patterns, and lateral STM manipulations demonstrate the feasibility of switching such weak-hydrogen-bonding patterns. The results would supplement the understanding of on-surface supramolecular self-assembly processes through weak intermolecular interactions and may also shed light on the rational design of artificial supramolecular architectures on solid surfaces.

The authors acknowledge the financial supports from the National Natural Science Foundation of China (21103128), the Shanghai "Shu Guang" Project supported by Shanghai Municipal Education Commission and Shanghai Education Development Foundation (11SG25), the Fundamental Research Funds for the Central Universities, the Research Fund for the Doctoral Program of Higher Education of China (20120072110045).

Notes and references

- College of Materials Science and Engineering, Tongji University, Caoan Road 4800, Shanghai 201804, P. R. China
E-mail: xurwei@tongji.edu.cn
† Electronic Supplementary Information (ESI) available: [supplementary STM images and DFT calculation results]. See DOI: 10.1039/b000000x/
‡ These authors contributed equally
- 1 Y.Ke, S.Lindsay, Y.Chang, Y.Liu and H.Yan, *Science*, 2008, **319**, 180.
 - 2 C. J. Baddeley, *Top. Catal.*, 2003, **25**, 17.
 - 3 S.Lei, J.Puigmarti-Luis, A.Minoia, M.Van der Auweraer, C.Rovira, R.Lazzaroni, D. B. Amabilino and S. De Feyter, *Chem. Commun.*, 2008, **6**, 703.
 - 4 T.Yokoyama, S.Yokoyama, T.Kamikado, Y.Okuno and S.Mashiko, *Nature*, 2001, **413**, 619.
 - 5 U.Schlickum, R.Decker, F.Klappenberger, G.Zoppellaro, S.Klyatskaya, M.Ruben, I. Silanes, A. Arnau, K. Kern, H. Brune and J. V. Barth, *Nano Lett.*, 2007, **7**, 3813.
 - 6 U. Schlickum, R. Decker, F. Klappenberger, G. Zoppellaro, S. Klyatskaya, W. Auwarter, S. Neppi, K. Kern, H. Brune, M. Ruben and J. V. Barth, *J. Am. Chem. Soc.*, 2008, **130**, 11778.
 - 7 R. E. A. Kelly, W. Xu, M. Lukas, R. Otero, M. Mura, Y. J. Lee, E. Lægsgaard, I. Stensgaard, L. N. Kantorovich and F. Besenbacher, *Small*, 2008, **4**, 1494.
 - 8 H.Kong, Q.Sun, L.Wang, Q.Tan, C.Zhang, K.Sheng and W.Xu, *ACS nano*, 2014, **8**, 1804.
 - 9 S.Karan, Y.Wang, R.Robles, N.Lorente and R.Berndt, *J. Am. Chem. Soc.*, 2013, **135**, 14004.
 - 10 S.De Feyter and F. C. De Schryver, *Chem. Soc. Rev.*, 2003, **32**, 139.
 - 11 W. Xu, H. Kong, C. Zhang, Q. Sun, H. Gersen, L. Dong, Q. Tan, E. Lægsgaard and F. Besenbacher, *Angew. Chem. Int. Ed.*, 2013, **52**, 7442.
 - 12 W. Xu, C. Zhang, H. Gersen, Q. Sun, H. Kong, L. Dong, K. Sheng, Q. Tan, E. Lægsgaard and F. Besenbacher, *Chem. Commun.*, 2013, **49**, 5207.
 - 13 S.Selvanathan, M. V. Peters, S. Hecht and L. Grill, *J. Phys.: Condens. Matter*, 2012, **24**, 354013.

-
- 14 D. Wang, Q. Chen and L. J. Wan, *PCCP*, 2008, **10**, 6467.
- 15 S. Weigelt, C. Busse, C. Bombis, M. M. Knudsen, K. V. Gothel, T. Strunskus, C. Wöll, M. Dahlbom, B. Hammer, E. Lægsgaard, F. Besenbacher and T. R. Linderoth, *Angew. Chem. Int. Ed.*, 2007, **119**, 9387.
- 5 16 S. Weigelt, C. Bombis, C. Busse, M. M. Knudsen, K. V. Gothel, E. Lægsgaard, F. Besenbacher and T. R. Linderoth, *ACS Nano*, 2008, **2**, 651.
- 17 F. Besenbacher, *Rep. Prog. Phys.*, 1996, **59**, 1737.
- 10 18 E. Lægsgaard, L. Österlund, P. Thostrup, P. B. Rasmussen, I. Stensgaard and F. Besenbacher, *Rev. Sci. Instrum.*, 2001, **72**, 3537.
- 19 M. Yu, W. Xu, Y. Benjalal, R. Barattin, E. Laegsgaard, I. Stensgaard, M. Hliwa, X. Bouju, A. Gourdon, C. Joachim, T. R. Linderoth and F. Besenbacher, *Nano Res.*, 2009, **2**, 254.
- 15 20 F. Rosei, M. Schunack, P. Jiang, A. Gourdon, E. Laegsgaard, I. Stensgaard, C. Joachim and F. Besenbacher, *Science*, 2002, **296**, 328.
- 21 G. Kresse and J. Hafner, *Phys. Rev. B*, 1993, **48**, 13115.
- 22 G. Kresse and J. Furthmüller, *Phys. Rev. B*, 1996, **54**, 11169.
- 23 P. E. Blöchl, *Phys. Rev. B*, 1994, **50**, 17953.
- 20 24 G. Kresse and D. Joubert, *Phys. Rev. B*, 1999, **59**, 1758.
- 25 J. P. Perdew, K. Burke and M. Ernzerhof, *Phys. Rev. Lett.*, 1996, **77**, 3865.
- 26 S. Grimme, *J. Comput. Chem.*, 2006, **27**, 1787.